

Quark and gluon jet spectra in $\gamma\gamma$ collisions

M.N.Dubinin

*Institute for Nuclear Physics, Moscow State University
119899 Moscow, Russia*

Abstract

We consider three jet production at high p_T in the $\gamma\gamma \rightarrow q\bar{q}g$ process and calculate quark and gluon jet spectra. The possibility of quark-gluon jet separation is discussed and compared with the $e^+e^- \rightarrow q\bar{q}g$ case.

1 Introduction

Three jet production in e^+e^- annihilation was investigated in details at PETRA and later at TRISTAN energies [1] in connection with the critical tests of perturbative QCD. In particular the difference between energy spectra of quark and gluon jets and quark and gluon jet multiplicities provided important information for quantitative tests of quantum chromodynamics.

Besides the studies of hadronic final state as a result of direct e^+e^- annihilation, the measurement of the two photon processes $e^+e^- \rightarrow e^+e^-X$ at PETRA and TRISTAN shows high physics potential. New tests are possible in LEP experiments, especially the precise measurement of the photon structure function and hadron production at high p_T [2]

At present time new experimental possibilities connected with the generation of γ beams by Compton backscattering of the laser beam on a high energy electron beam [3] are discussed extensively [4]. Investigation of the jet phenomena in $\gamma\gamma$ collisions at the energy of several hundred GeV is one of the most interesting questions for $\gamma\gamma$ colliders phenomenology.

In this paper we discuss three jet production in the region of large p_T originated from t-channel quark exchange between the colliding photons. At next linear colliders energy there are two other possible mechanisms for the jet production in high p_T region with the cross sections of the same order [5]: (1) gluon exchange between two pairs of quark jets (2) W^+W^- boson production. However, they have different final state topologies and can easily be distinguished from the mechanism under consideration. At smaller p_T the photon looks more like the hadron-like object and special treatment beyond the simple QCD tree approximation is necessary.

The aims of this paper are the calculation of high p_T quark and gluon jets energy spectra in $\gamma\gamma$ collisions and comparison of the results with the e^+e^- case.

2 Quark and gluon jet spectra in the process

$$\gamma\gamma \rightarrow q\bar{q}g$$

The first order QCD calculation for three jet production in $e^+e^- \rightarrow q\bar{q}g$ ($q = u, d, s$) gives the following well-known result for the spectra [6]:

$$\frac{d\sigma}{dz_1 dz_2} = \frac{16\pi\alpha^2\alpha_s}{9} \frac{1}{s} \frac{z_1^2 + z_2^2}{(1-z_1)(1-z_2)} \quad (1)$$

where z_1, z_2, z_3 are the energy fractions of quark, antiquark and gluon

$$z_1 = \frac{2E_{\bar{q}}}{\sqrt{s}}, \quad z_2 = \frac{2E_q}{\sqrt{s}}, \quad z_3 = \frac{2E_g}{\sqrt{s}} \quad (2)$$

satisfying the equality

$$z_1 + z_2 + z_3 = 2 \quad (3)$$

Distribution (1) defines the topology of the final state (or topology of the primary process) in e^+e^- collision. Since quarks and gluons are unobservable, in the following various fragmentation models are used to generate real event samples. However, event generation will be beyond our analysis at present stage.

The calculation in e^+e^- case for two Feynman amplitudes only (gluon is radiated from quark or antiquark leg) is not technically difficult. In $\gamma\gamma$ case we have 6 amplitudes represented in Fig.1. Symbolic calculation for the

corresponding 21 squared amplitudes could be more complicated. However, it is much simplified because the compact form of the result for the sum of 21 squared diagrams can be obtained [7]:

$$|M|^2 = \frac{64}{27} e^4 g_s^2 (p_4 p_5) \frac{\sum_{i=1}^3 (p_i p_4)(p_i p_5)[(p_i p_4)^2 + (p_i p_5)^2]}{\prod_{i=1}^3 (p_i p_4)(p_i p_5)} \quad (4)$$

We reproduced this formula using CompHEP package [8] for generation of symbolic result and REDUCE system [9] in the following algebraic transformations.

For the process $\gamma(p_1)\gamma(p_2) \rightarrow q(p_4)\bar{q}(p_5)g(p_3)$ we are using the kinematical variables

$$\cos\vartheta_{14}^*, \quad z_1, \quad z_2, \quad \lambda \quad (5)$$

where $\cos\vartheta_{14}^*$ is the angle between particle 1 and particle 4 in the c.m.s. of (1,2), λ is the helicity angle between the planes (1,4) and (3,4) in the c.m.s. of (3,5). The phase space in these variables takes the form

$$dR_3 = \frac{1}{1024\pi^4} dz_1 dz_2 d\cos\vartheta_{14}^* d\lambda \quad (6)$$

In the case of $e^+e^- \rightarrow q\bar{q}g$ process the matrix element has collinear singularities only. In the case of $\gamma(p_1)\gamma(p_2) \rightarrow q(p_4)\bar{q}(p_5)g(p_3)$ process additional t-channel singularity appears. The denominator of the squared amplitude contains four momenta products (see more details in the Appendix)

$$p_1 p_4 = z_2 \frac{s}{4} (1 - \cos\vartheta^*) \quad (7)$$

$$p_1 p_3 = \frac{s}{4z_2} (a_1 - b_1 \cos\lambda) \quad (8)$$

$$p_2 p_5 = \frac{s}{4z_2} (a_4 - b_1 \cos\lambda) \quad (9)$$

where

$$a_1 = \cos\vartheta^* (z_2^2 + z_1 z_2 - 2z_1 - 2z_2 + 2) + z_2 (2 - z_1 - z_2) \quad (10)$$

$$a_4 = -\cos\vartheta^* (-z_1 z_2 + 2z_1 + 2z_2 - 2) + z_1 z_2 \quad (11)$$

$$b_1 = 2\sin\vartheta^* \sqrt{(1 - z_1)(1 - z_2)(z_1 + z_2 - 1)} \quad (12)$$

Integration over λ leads to the structures $\sqrt{a_1^2 - b_1^2}$ and $\sqrt{a_4^2 - b_1^2}$ in the denominator (see more details in Appendix). For this reason besides the poles of matrix element for the scattering in forward-backward directions (no gluon emission from final quark) there are parametrically dependent poles at

$$|\cos\vartheta^*| = \frac{2(z_1 + z_2 - 1) - z_1 z_2}{z_1 z_2} \quad (13)$$

corresponding to the t-channel singularity in the diagrams with gluon emission from the quark leg. (In this case the antiquark is emitted in the opposite hemisphere at zero angle). While integrating over $\cos\vartheta^*$ we introduced kinematical cuts ϵ_1 and ϵ_2 for quark near the forward pole and the poles defined by (13). After two integrations over the angular variables $\cos\vartheta^*$, λ we obtain the following result for three jet spectra in $\gamma\gamma$ collisions:

$$\begin{aligned} \frac{d\sigma}{dz_1 dz_2} = & \frac{e^4 g^2}{27\pi^2} \frac{1}{s} \frac{1}{z_1^2 z_2^2 (1 - z_1)(1 - z_2)} \{ z_1^2 z_2^2 [(1 - z_1)^2 + (1 - z_2)^2] \\ & \times [\ln \frac{1}{2\epsilon_1 \epsilon_2^2} + 2 \ln \frac{\omega_1 \omega_2}{z_1 z_2} - \frac{2(z_1 + z_2 - 1) - z_1 z_2}{z_1 z_2} \ln \frac{\omega_1}{\omega_2}] \\ & + z_1^2 ((1 - z_1)^2 (1 - z_2)^2 + z_2^4) \ln \frac{2}{\epsilon_1} \\ & + z_2^2 ((1 - z_1)^2 (1 - z_2)^2 + z_1^4) \ln \frac{\omega_1 \omega_2}{\epsilon_2^2} \\ & + 2 z_1^2 z_2^2 (z_1^2 + z_2^2) \ln \frac{\omega_1}{2 z_1 z_2} \\ & + z_1^4 z_2 + z_1 z_2^4 - 5 z_1^3 z_2 - 5 z_1 z_2^3 + 4 z_1^2 z_2 + 4 z_1 z_2^2 + z_1^2 z_2^3 + z_1^3 z_2^2 \\ & + 4 z_1^3 + 4 z_2^3 - 4 z_1^2 z_2^2 - 2 z_1^2 - 2 z_2^2 - 2 z_1^4 - 2 z_2^4 \} \end{aligned} \quad (14)$$

where

$$\omega_1 = 2(z_1 + z_2 - 1) = 2(1 - z_3) \quad (15)$$

$$\omega_2 = 2(1 - z_1)(1 - z_2) \quad (16)$$

Besides the collinear singularities in $\gamma\gamma$ case the spectrum (14) has the factor $(z_1 z_2)$ in denominator and logarithmic terms originating from t-channel quark exchange. Kinematical cut for ϵ_1 in the case of nonzero fermion masses is $2m_q/\sqrt{s}$, it is easy to show that the cut for ϵ_2 is of the same order.

3 Quark and gluon jet separation

We show double differential spectra of quark and gluon jets in e^+e^- and $\gamma\gamma$ collisions ((1),(14)) at the energy scale $\sqrt{s} \sim 10^2 GeV$ in Fig.2. In the $\gamma\gamma$ case the cross section is an order of magnitude larger than for e^+e^- case. The shape of the spectra are similar.

In the case when there are no additional methods of quark and gluon jet identification the spectra are not measurable separately and the usual way of analysis is jet ordering in energy. In Fig.3 we show single differential spectra of quark and gluon jets in the case of e^+e^- and $\gamma\gamma$ collisions. In the e^+e^- case quark and gluon jet spectra show large difference giving the possibility of good jet discrimination. For instance, about 70% of the jets at z less than 1/3 are gluon jets and about 50% of the jets at z between 0.6 and 0.9 are quark jets. In the $\gamma\gamma$ case the difference between the spectra is also well pronounced and identification possibilities of the quark and gluon jets by energy ordering seem not worse than for e^+e^- case. Improvement of jet identification in some experimental situations could be provided by flavor tagging [10] or comparison of $q\bar{q}g$ and $q\bar{q}\gamma$ event topologies [1]. Probably some combination of different methods can give optimal results.

Acknowledgements

The author is grateful to M.Fontannaz, J.Fujimoto, J.P.Guillet, K.Kato, T.Munehiza and Y.Shimizu for useful comments and discussions. The work was partially supported by ISF (grant M9B000) and INTAS (grant 93-1180, contract 1010-CT93-0024).

Appendix

In this section we shall show some details of the calculation taking squared amplitudes (1) and (5) (see Fig.1) as an example.

Four momenta products in the variables (5) have the form

$$\begin{aligned} p_1 p_2 &= \frac{s}{2} \\ p_3 p_4 &= \frac{s}{2}(1 - z_1) \end{aligned}$$

$$\begin{aligned}
p_3 p_5 &= \frac{s}{2}(1 - z_2) \\
p_4 p_5 &= \frac{s}{2}(z_1 + z_2 - 1) \\
p_1 p_4 &= z_2 \frac{s}{4}(1 - \cos\vartheta^*) \\
p_2 p_4 &= z_2 \frac{s}{4}(1 + \cos\vartheta^*) \\
p_1 p_3 &= \frac{s}{4z_2}(a_1 - b_1 \cos\lambda) \\
p_1 p_5 &= \frac{s}{4z_2}(a_2 + b_1 \cos\lambda) \\
p_2 p_3 &= \frac{s}{4z_2}(a_3 + b_1 \cos\lambda) \\
p_2 p_5 &= \frac{s}{4z_2}(a_4 - b_1 \cos\lambda)
\end{aligned}$$

where

$$\begin{aligned}
a_1 &= \cos\vartheta^*(z_2^2 + z_1 z_2 - 2z_1 - 2z_2 + 2) + z_2(2 - z_1 - z_2) \\
a_2 &= \cos\vartheta^*(-z_1 z_2 + 2z_1 + 2z_2 - 2) + z_1 z_2 \\
a_3 &= -\cos\vartheta^*(z_2^2 + z_1 z_2 - 2z_1 - 2z_2 + 2) + z_2(2 - z_1 - z_2) \\
a_4 &= -\cos\vartheta^*(-z_1 z_2 + 2z_1 + 2z_2 - 2) + z_1 z_2 \\
b_1 &= 2\sin\vartheta^* \sqrt{(1 - z_1)(1 - z_2)(z_1 + z_2 - 1)}
\end{aligned}$$

It is worth noticing that this set is not invariant under the transposition $z_1 \leftrightarrow z_2$ (as long as we are using the $\bar{q}g$ c.m.s. as the reference frame). The matrix element has the symmetry $quark \leftrightarrow antiquark$, so this symmetry must be restored in the final result for the spectra (at least in the nondivergent terms, artificial cuts near the poles can break the symmetry). Squared diagrams (1) and (5) sum

$$\frac{128}{81} e^4 g_s^2 \left(\frac{p_1 p_3}{p_1 p_5 p_3 p_4} + \frac{p_2 p_3}{p_2 p_4 p_3 p_5} \right)$$

after the integration over the helicity angle λ takes the form

$$\frac{d\sigma}{dz_1 dz_2 \cos\vartheta^*} = \frac{256}{81s} e^4 g_s^2 \frac{-2(a_1 + a_2) \sqrt{a_2^2 - b_1^2} \arctg(\sqrt{\frac{a_2 - b_1}{a_2 + b_1}} \operatorname{tg}(\lambda/2)) + \lambda(a_2^2 - b_1^2)}{(a_2^2 - b_1^2)(z_1 - 1)}$$

where

$$\sqrt{a_2^2 - b_1^2} = 2|z_1 z_2 (\cos\vartheta^* - 1) + 2(z_1 + z_2 - 1)|$$

Integration over $\cos\vartheta^*$ must take into account two cases for the sign of the absolute value. The physical region of the reaction $\gamma\gamma \rightarrow q\bar{q}g$ in z_1, z_2 plane is the triangle with vertices $(0,1);(1,0);(1,1)$. Hyperbola reflecting the relation between $\cos\vartheta^*, z_1, z_2$ for t-channel pole (13) crosses the physical region from $(0,1)$ to $(1,0)$ (see Berends et.al in [7]). Integration of the rational function

$$\begin{aligned} \frac{d\sigma}{dz_1 dz_2 d\cos\vartheta^*} = & \frac{128\pi e^4 g_s^2}{81s} \left\{ 2 \frac{2z_2 - z_2^2 + z_2^2 \cos\vartheta^*}{|z_1 z_2 (1 - \cos\vartheta^*) - 2(z_1 + z_2 - 1)|(1 - z_1)} \right. \\ & \left. - \frac{2}{1 - z_1} + \frac{\cos\vartheta^* (z_2^2 + z_1 z_2 - 2z_1 - 2z_2 + 2) + z_2 (2 - z_1 - z_2)}{(1 - \cos\vartheta^*)(1 - z_2)z_2^2} \right\} \end{aligned}$$

gives the result for the spectrum

$$\begin{aligned} \frac{d\sigma}{dz_1 dz_2} = & \frac{e^4 g_s^2}{81\pi^2 s} \frac{1}{z_1^2 z_2^2 (1 - z_1)(1 - z_2)} \\ & [z_2^2 (1 - z_2)^2 \ln(\frac{\omega_1 \omega_2}{\epsilon_2^2}) + z_1^2 (1 - z_1)^2 \ln(\frac{2}{\epsilon_1}) \\ & + z_1^2 z_2^2 (z_1 + z_2 - 1) + (z_1^2 (1 - z_1) + z_2^2 (1 - z_2))(2z_1 + 2z_2 - 2 - z_1 z_2)] \end{aligned}$$

Calculation for the sum of 21 squared diagrams gives the same symbolic structures.

References

- [1] Collected physics papers (I) of TRISTAN experiments, KEK, Tsukuba, 1994

- [2] P. Aurenche, A. Douiri, R. Baier, M. Fontannaz, D. Schiff, in: *Physics at LEP*, ed.by J.Ellis,R.Peccei, CERN report 86-02, 1986
- [3] I. Ginzburg, G. Kotkin, V. Serbo, V. Telnov, Nucl.Instr.Meth. 205 (1983) 147
- [4] E. Boos, M. Dubinin, V. Ilyin, A. Pukhov, in: *e^+e^- collisions at 500 GeV: the physics potential*, ed.by P.Zerwas, DESY report 93-123C, 1993, p.561
- [5] I. Ginzburg, D. Ivanov, V. Serbo, in: *Proc.of Workshop on Physics and Experiments with Linear e^+e^- Colliders*, ed.by F.Harris, S. Olsen, S. Pakvasa, X.Tata, World Scientific, Singapore, 1993, p.600
- [6] J. Ellis, M.K. Gaillard, G.G. Ross, Nucl.Phys.B111 (1976) 253
T.A. DeGrand, Y.J. Ng, S.H.H. Tye, Phys.Rev.D16 (1977) 3251
A. DeRujula, J. Ellis, E.G. Floratos, M.K. Gaillard, Nucl.Phys.B138 (1978) 387
G. Kramer, G. Schierholz, Phys.Lett.82B (1979) 102
P. Hoyer, P. Osland, H.G. Sander, T.F. Walsh, P.M. Zerwas, Nucl. Phys. B161 (1979) 349
S. Nandi, W. Wada, Phys.Rev.D21 (1980) 76
H.P. Nilles, K.H. Streng, Phys.Rev.D23 (1981) 1944
- [7] F. Berends, Z. Kunszt, G. Gastmans, Phys.Lett.92B (1980) 186,
Nucl.Phys.B182 (1981) 397
P. Aurenche, A. Douiri, R. Baier, M. Fontannaz, D. Schiff, Z.Phys.C24 (1984) 309
- [8] E. Boos et.al.,in: *'91 Electroweak Interactions and Unified Theories (Proc. of the XXVIth Rencontre de Moriond)*, ed.by J. Tran Than Van, Editions Frontieres, 1991, p.501
E. Boos et.al.,in: *New Computing Techniques in Physics Research II (Proc. of the Second Int.Workshop on Software Engineering, Artificial Intelligence and Expert Systems in High Energy and Nuclear Physics)*, ed.by D. Perret-Gallix, World Scientific, 1992, p.665
E. Boos, M. Dubinin, V. Ilyin, A. Pukhov, V. Savrin, preprint INP MSU 94-36/358, 1994 (**hep-ph/9503280**)
- [9] REDUCE by A.C. Hearn, RAND Corp., CP78 (rev.7.91), 1991

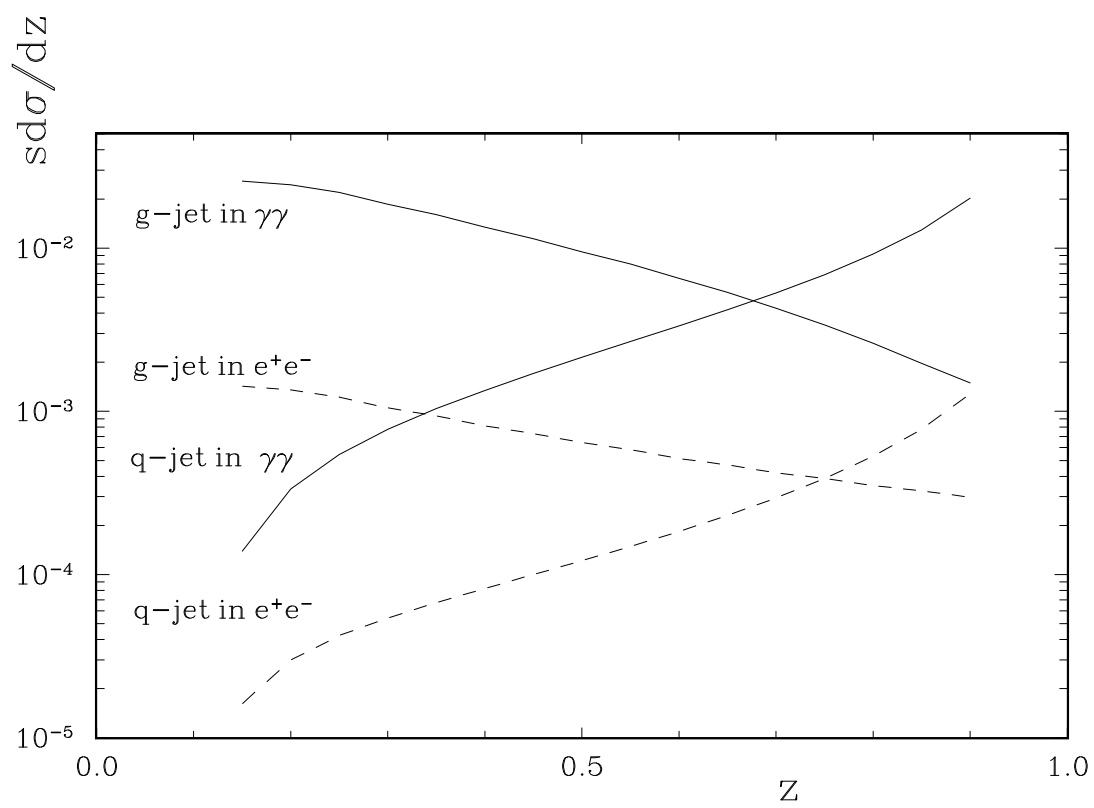
- [10] H. Borner, P. Grosse-Wiesmann, in: *e^+e^- collisions at 500 GeV: the physics potential*, ed.by P. Zerwas, DESY report 92-123A, 1992, p.63

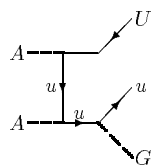
Figure captions

Fig.1 Feynman diagrams for $\gamma\gamma \rightarrow q\bar{q}g$.

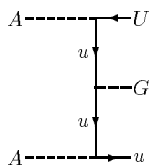
Fig.2 Double differential spectra $s d\sigma/dz_1 dz_2$ at fixed $z_2 = 0.9$ of parent quark and gluon in the reactions $e^+e^- \rightarrow q\bar{q}g$ and $\gamma\gamma \rightarrow q\bar{q}g$ ($q = u$). $\epsilon_1 = \epsilon_2 = 10^{-5}$, $e = 0.313$, $g_s = 1.59$

Fig.3 Differential spectra $s d\sigma/dz_2$ (integrated over z_1) of parent quark and gluon in the reactions $e^+e^- \rightarrow q\bar{q}g$ and $\gamma\gamma \rightarrow q\bar{q}g$ ($q = u$).

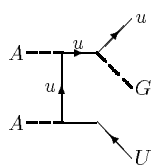




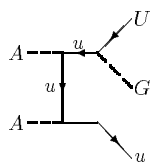
diagr.1



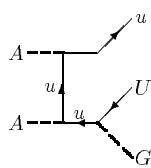
diagr.2



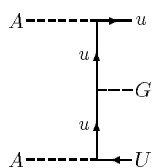
diagr.3



diagr.4



diagr.5



diagr.6

